

# **$^3\text{He}/^4\text{He}$ Pulse Tube Cryocooler Performance Optimization**

**M. Lewis<sup>1</sup>, R.P. Taylor<sup>1,2</sup>, P.E. Bradley<sup>1</sup>, and R. Radebaugh<sup>1</sup>**

<sup>1</sup>National Institute of Standards and Technology  
Boulder, CO 80305 USA

<sup>2</sup>Virginia Military Institute  
Lexington, VA 24450 USA

## **ABSTRACT**

A single-stage pulse tube cryocooler capable of using either  $^3\text{He}$  or  $^4\text{He}$  as the working fluid was designed to achieve its refrigeration power at 4.2 K when energized by a 30 Hz pressure wave generator. By design, this system is unique, as an active expander is utilized to achieve the desired cold end phase angle for maximizing refrigeration power. Initial results from this system showed poor performance related to non-ideal thermal stratification in the pulse-tube component. Due in part to this larger than expected pulse-tube loss, performance goals were not achieved. This paper addresses work performed relative to optimization of the pulse tube component and associated transitions in a 4 K pulse tube cryocooler using  $^3\text{He}$  and  $^4\text{He}$  as working fluids to achieve the desired operational characteristics. This optimization was performed using a commercial CFD solver coupled with design models for the regenerator, expander, and heat exchanger performance. Based upon the fluid dynamic modeling results, the geometries of the pulse tube and associated transition components were modulated. The performance impact of these system changes is reported for the case of  $^4\text{He}$  as the working fluid.

## **INTRODUCTION**

To attain reliable and efficient cryocooler operation for many applicable fields, miniaturization must be achieved for the 4 Kelvin Pulse Tube Cryocooler (PTC). This miniaturization is being driven by the technologies enabled via cryogenic cooling such as superconducting electronics, defense applications, spacecraft cooling, and advanced imaging platforms (IR and Terahertz). In each of these applications 4 K cryogenic cooling is the enabling technology, but is problematic from a system design/integration standpoint. The difficulty and problems associated with the current state of the art in 4 K cryocoolers is related to three specific areas: 1) large physical sizes, 2) high vibration levels, and 3) low cooling powers.

Mitigation of physical size in regenerative cryocoolers can be achieved through three mechanisms: reduction of pressure wave generator size, use of higher frequency, and minimizing the volume of the phase shifting mechanisms.

Work by Radebaugh<sup>1</sup> has shown that increased operational frequency lends well to increased power density. An added benefit to this approach is a reduction in compressor volume reducing

physical size. Reduction of size via phase shifting mechanisms is unique at 4 K. In general, moderate temperature cryocoolers (40-80 K) utilize an inertance tube to provide desired phase relationships in the PTC. However, use of inertance tubes at 4 K is problematic due to the lack of attainable phase arising from acoustic powers flows on the order of watts. Recent work by Radebaugh<sup>2</sup> has shown the potential for using a room temperature expander coupled through a secondary regenerator or regenerator pulse tube combinations. Work by Lewis et al.<sup>3</sup>, has documented the use of a commercial linear compressor operated as an expander at a nominal temperature of 35 K. Both of these cases are relevant, as essentially infinite phase is attainable, phase modulation is realized in real time, and the system size is considerably reduced compared to an inertance network.

In regard to vibration, regenerative cryocoolers will inherently always have some measurable level of vibration. These vibration sources, typically large for GM based systems, arise from the low frequency operation of the motor in the cooler head and the moving expander in the cold end. Mitigation of the motor vibration has been achieved by various manufactures through use of a split design where the motor is de-coupled from the cold head but at the expense of increased physical size. Reduction of the cold end vibration levels has been achieved via development of GM based Pulse Tube Cryocoolers that remove the moving cold displacer. In any case, there is vibration due to the pressure oscillation inside the system that is unavoidable.

Low cooling power for 4K PTC's is not a new problem, but recent work has shown many ways to increase the cooling power. Such ways include the use of new novel rare ceramic paramagnetic materials for the regenerator matrix, use of reduced charge pressure, higher operational frequencies, 30 Hz limit for current regenerator material sizes, and use of  $^3\text{He}$  in place of  $^4\text{He}$  as the working fluid. Recent work at NIST by Garaway et al.<sup>4</sup> has documented the development of the miniaturized  $^3\text{He}/^4\text{He}$  Pulse Tube Cryocooler (PTC) shown in Figures 1 and 2. This cooler was designed to allow for efficient operation, small size, and could be operated with both  $^3\text{He}$  and  $^4\text{He}$  working fluids —  $^3\text{He}$  allowing for higher cooling power and efficiency. Initial results from this test facility

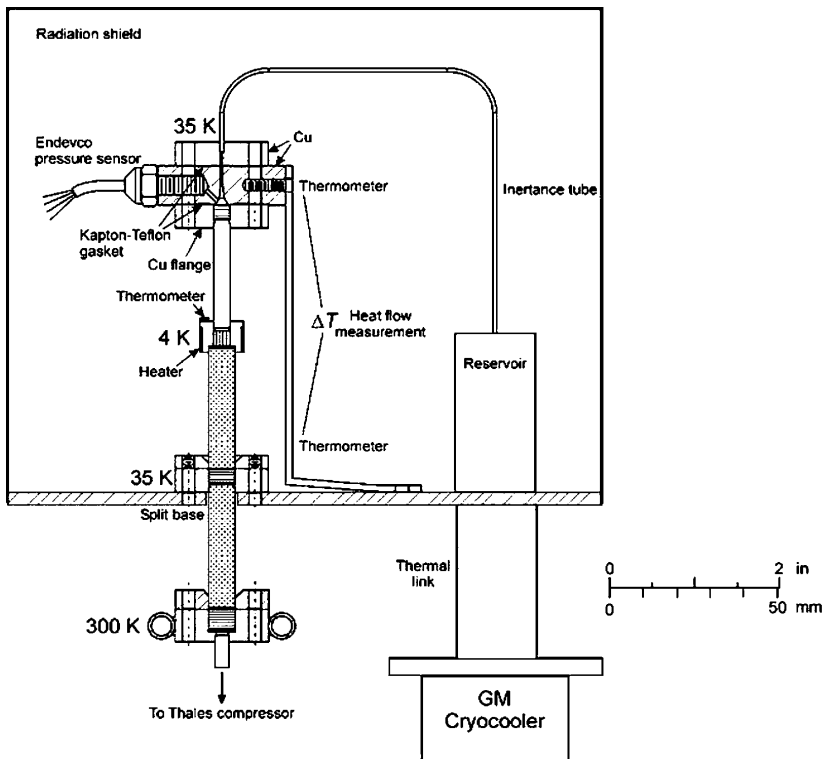
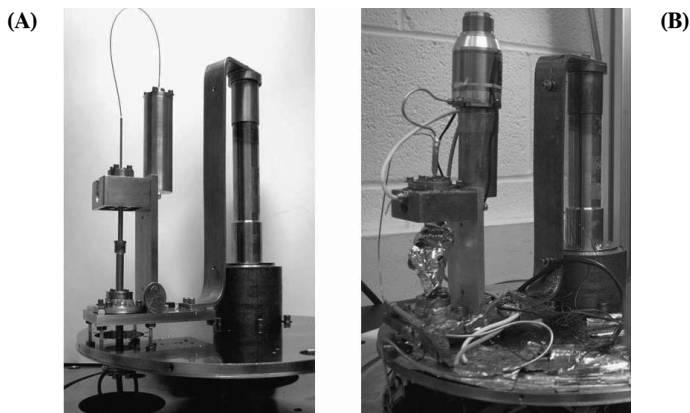


Figure 1. Schematic of the original test facility design configuration.



**Figure 2.** Photos showing (A) the original constructed test facility, and (B) the final test facility configuration utilizing a cold expander at 35 K.

indicated a potential problem with phase shifting being less than ideal, yielding no-load temperatures of 6.1 K ( $^4\text{He}$ ) and 5.2 K ( $^3\text{He}$ ) at a charge pressure of 0.8 MPa and a frequency of 16 Hz. In each case, the no-load temperatures are considerably higher than the 4.2 K design objective. Methods used by Garaway to achieve a more ideal phase shift included use of a double inlet configuration, modification of the pulse tube by restricting its diameter via a G10 insert, and use of a linear expander at the pulse tube warm end. Of these system modifications, only use of the linear expander provided useful results.

Recent measurements using the test facility described by Garaway<sup>4</sup> have yielded less than ideal results as the initial data have been unrepeatable. Recent measurements discussed by Lewis et al.<sup>3</sup> indicated a minimum temperature of 9.6 K ( $^4\text{He}$ ) was achieved at the same charge pressure and frequency. Use of a cold expander did allow for phase modulation, yet the results from Garaway<sup>4</sup> and Lewis<sup>3</sup> were less than ideal. This is due to optimum system performance being identified at 16 Hz compared to the 30 Hz design frequency. In all cases, it has become clear that there are significant losses impacting the system performance. Current ideas regarding this lack of system performance include potential problems with the regenerator matrix configuration, less than ideal impedance matching, and poor thermal communication between the working fluid and the wire mesh heat exchangers at the cold and warm ends of the pulse tube. Based on the initial results that indicated poor phase shifting performance coupled with off design operating frequency, the pulse tube and warm end heat exchanger was identified for modification. This was chosen as poor thermal performance of this heat exchanger can significantly impact the phase shifting characteristics (gas at higher temperature than sensor reports) and would significantly impact the thermal performance of the pulse tube component. The remainder of this paper details the modifications performed and their impact on system performance.

## COMPUTATIONAL FLUID DYNAMIC DESIGN

To aid in selection of new, potential design improvements, analysis using a commercial CFD package was performed. This CFD model is 2D axisymmetric and detailed specifications and methodology are described in more detail by Taylor.<sup>5</sup> The primary differences between the current approach and that previously reported by Taylor are noted below:

1. Use of a quasi-real gas model for the working fluid  $^4\text{He}$ . This gas model treated the density as real gas based using the Redlich-Kwong equation of state, the specific heat at constant pressure as a constant at 3kJ/kg-K, and the dynamic viscosity and thermal conductivity were modeled using polynomial fits to data over the range of 3-50 K via Engineering Equation Solver.<sup>6</sup>
2. Use of the k- $\omega$  SST closure model for turbulence modeling. This model is applicable to the class of internal flow present in a PTC.

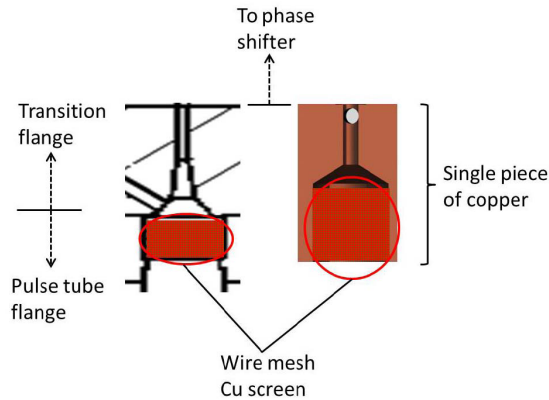


**Figure 3.** Illustration showing (Left) the original test facility warm heat exchanger configuration and (Right) the re-designed warm end heat exchanger configuration.

### 3. Neglected the thermal interaction between the wall material and the working fluid.

The developed CFD models possessed spatial discretization sufficiently refined to capture relevant flow features while temporal discretization was defined at 400 steps/cycle. The relevant outputs from the CFD model for this investigation included the time averaged temperature profile and the turbulent intensity at the cycle end.

## EXPERIMENTAL HARDWARE PERMUTATIONS

The sections below detail the specific design permutations that were implemented based on the original experimental observations, heat exchanger modeling using ISOHX<sup>7</sup>, and CFD simulations of the hydraulic profiles. Initial emphasis is placed on the pulse tube warm heat exchanger configuration followed by pulse tube geometric modulation.

### Heat Exchanger Configuration

Due to performance degradation noted by Lewis<sup>3</sup> relative to prior results described by Garaway<sup>4</sup>, it was theorized that poor performance could be attributed to low heat rejection at the pulse tube warm heat exchanger. Specifically, due to the system set-up, it is plausible that temperature readings being taken were not accurate with respect to the time averaged working fluid temperature. This poor thermal performance was attributed to the relatively resistive thermal heat rejection path. Specifically, the heat exchanger core was located in a 304 Stainless steel flange that was bolted to the primary copper thermal rejection flange. In this case, heat rejection was to occur across a contact resistance between the two bolted flanges. Additional concerns with this design were related to the relatively steep geometric gradient present in the flow transitions potentially leading to jetting effects in the heat exchanger core and pulse tube component. This original configuration is shown in Figure 3 (left).

Due to these potential sources of losses, the warm end heat exchanger was redesigned. This redesign was accomplished using ISOHX and the previously discussed CFD model. This new design and original design are illustrated in Figure 3. Analysis using ISOHX was relatively straightforward and was primarily used to ensure adequate heat transfer using similar flow conditions as the original model. The initial CFD model results for the time-averaged temperature profiles in the pulse tube were used to determine any gross flow mal-distribution. The temperature contours for the original and new configuration are shown in Figure 4. Observation of the results presented in Figure 4 illustrate that both designs maintain relatively decent thermal stratification in the pulse tube component. As the results of this analysis did not clearly note any potential flow features, even considering the relatively significant geometric changes, an additional flow parameter was investi-

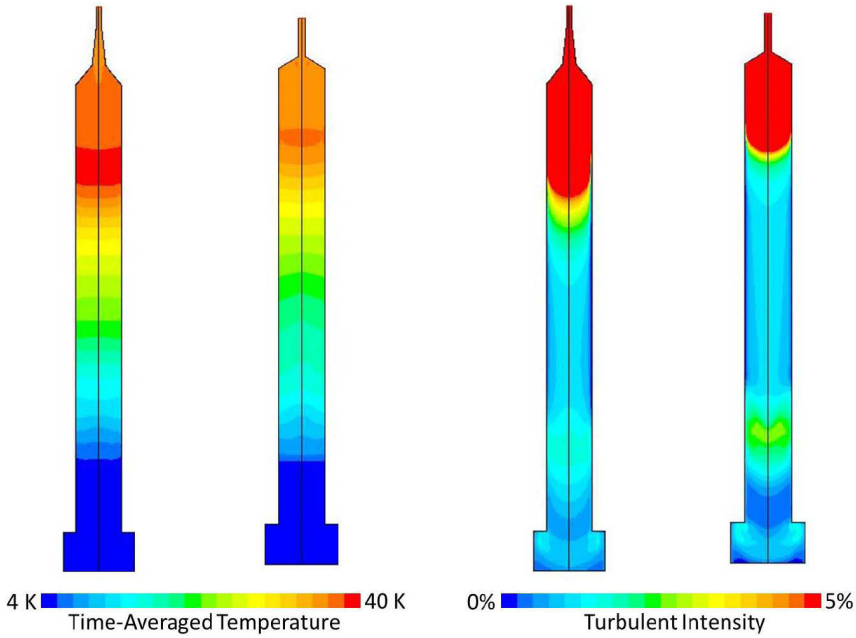


**Figure 4.** Illustrations showing the turbulent intensity profile in the pulse tube for (Left) the original heat exchanger configuration, and (Right) for the re-designed heat exchanger configuration.

gated. This parameter was the level of turbulent intensity in the flow field at the end of a given cycle. The turbulent intensity is generally considered a measure of the relative level of turbulence present and can be expressed as,

$$TI = \frac{u'}{U} \quad (1)$$

where  $u'$  is the Root-mean-square of the random turbulent velocity perturbations and  $U$  is the Reynolds averaged flow velocity. Turbulence in the pulse tube component generally arises from improper warm-end flow transitioning. In many ways, the turbulent intensity can illustrate problems not easily uncovered through temperature profile observation alone. The results of this analysis are illustrated in Figure 4.

As shown in Figure 4, there is a clear distinction between the turbulence level in the pulse tube component for the original configuration and the redesigned configuration. The original configuration contained an inadequate flow transition, resulting in a high level of pulse tube turbulence resulting from jet like effects. The re-designed configuration, while still possessing some level of turbulence, has a lower intensity level due to adequate flow transitioning.

### Pulse Tube Geometry

As Garaway noted in his work, enhanced phase performance was achieved via modulation of the pulse tube aspect ratio. Due to this noted effect, secondary efforts of this work focused on optimization of the system performance using alternative pulse tube designs using CFD. This effort was guided by the methods discussed by Taylor in regard to the sizing of the pulse tube for a fixed volume; 6x the swept volume is used in all cases discussed. Based on work by Taylor, the pulse designs were quantified terms of a non-dimensional pulse tube diameter expressed as,

$$\bar{D}_{PT} = \frac{D_{PT} - D_{IN}}{D_{REG} - D_{IN}} \quad (2)$$

**Table 1.** Pulse tube geometric specifications

Parameter	Design 1 (Original)	Design 2	Design 3
ID (mm)	3.55	2.87	2.083
Length (mm)	26.7	42.6	81
ND diameter (-)	0.55	0.35	0.19



**Figure 5.** Plot showing the constructed pulse tube designs.

where  $D_{PT}$  is the diameter of the pulse tube,  $D_{REG}$  is the diameter of the regenerator, and  $D_{IN}$  is the diameter of the inertance tube (or expander connection line in this case). Past CFD modeling work has shown that for a pulse tube volume that is 5-6x the cold regenerator gas swept volume, the ideal non-dimensional diameter is roughly 0.2. Using the original design information for the system, it was determined the original pulse tube configuration was far from this optimum with a  $\bar{D}_{PT} \sim 0.5$  (Design 1). Based on this information, two new designs were developed that had non-dimensional diameters of 0.19 (Design 3) and 0.35 (Design 2). The geometric dimensions of the original and new pulse tube designs are summarized in Table 1, and the physical size of the three as-constructed pulse tube permutations is shown in Figure 5.

Using the information provided in Table 1, coupled with information regarding the regenerator and connecting lines dimensions, representative CFD models were created that modeled all components from the regenerator exit to the entrance of the convection line. Modeling inputs and specifications are noted in Table 2. Note all of these configurations used the new heat exchanger configuration discussed previously. As discussed previously, the main results of interest were the time-averaged temperature profiles and the turbulent intensity. The results from this analysis are presented in Figure 6.

As shown in Figure 6, the temperate profiles of all three pulse tube configurations remain relatively stratified. In the case of the longer pulse tube designs, there is a more defined buffer regions for the gas “piston” to transverse during the course of a cycle. Furthermore, the higher temperatures are further removed from the cold end heat exchanger aiding in thermal isolation and increased cooling capacity. However, further observation of the flow using the turbulent intensity

**Table 2.** Pulse tube geometric specifications

Parameter	Symbol	Nominal Value
Mean system pressure	$\bar{P}$	1.0 MPa
Pressure ratio (cold end)	$PR$	1.5
Frequency	$f$	30 Hz
Cold end temperature	$T_c$	4 K
Warm end temperature	$T_h$	35 K
Mass flow rate	$\dot{m}$	0.37 g/s
Cold end phase angle	$\theta$	-30°

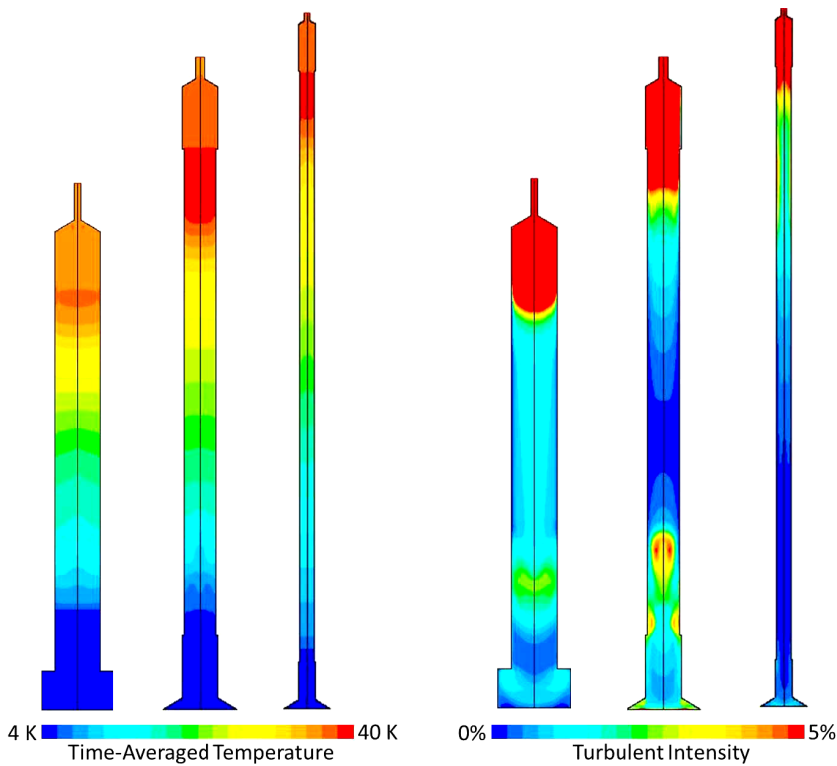


**Figure 6.** Photo illustrating the constructed pulse tube permutations with aspect ratios of 0.31, 0.37, and 0.55 utilizing the new heat exchange configuration.

provides more insight into the flow profile. The original configuration contained an inadequate flow transitioning resulting in a high level of pulse tube turbulence resulting from jet like effects. The re-designed configurations, while still possessing turbulence at transition locations, remain essentially turbulence free near the center of the pulse tube aiding in efficient enthalpy transport. Note that the turbulence regions are further reduced as the ND diameter is decreased. These results indicate the new pulse tube designs at the lower ND diameters should perform better than the original design.

**EXPERIMENTAL RESULTS**

The pressure oscillator used to drive the third stage hybrid and an expander connected to the hybrid warm-end pulse tube, one located at room temperature and the other at 35 K, were operated at a specific frequency by use of two signal generators. One of the signal generators sent a 10 MHz clock signal to the other in order to phase-lock the two instruments and subsequently phase-lock the pressure oscillator and the expander. These phase-locked signals were amplified with two separate power amplifiers that were used to operate the oscillator and the expander at specified, and separate, electrical input powers. The input power to the system pressure oscillator was typically run at the maximum power of the compressor. The electrical power to the expander was adjusted to obtain specific low-end temperature results. Once the input power was set, the phase offset was adjusted to the expander relative to that of the system pressure oscillator. Offset phase angles from 0 to 360 degrees were used in the measurements.

Initial experiments using the original design components were taken to obtain no-load low-end temperatures at 30 Hz, 24 Hz and 16 Hz. The offset phase was adjusted using the signal generators to achieve the low-end temperatures by obtaining the desired phase angle. These low-end tempera-

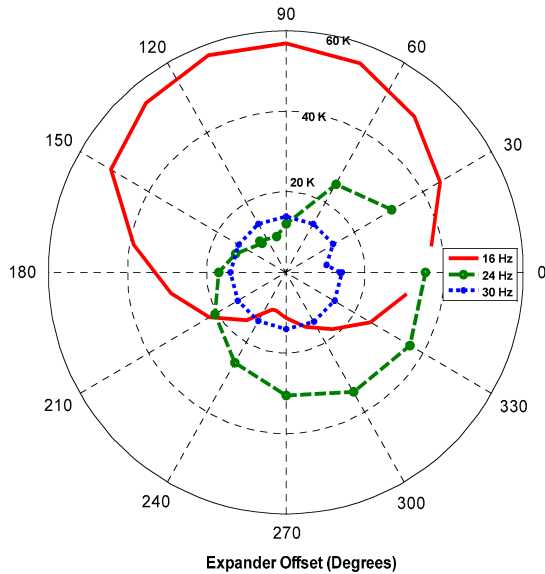


**Figure 7.** Plot showing no-load temperature of the original system as a function of operating frequency and the expander offset angle; charge pressure is 1 MPa.

tures were 13.0 K, 10.4 K and 9.7 K, respectively. The current at the expander was 1.7A, 1.8A and 2.9A for the corresponding frequencies. Once the low-end temperature was determined, the offset frequency was changed to observe the phase angle effects on the low-end temperature. These results are shown in Figure 7. Although the optimum design frequency was 30 Hz the best low-end temperature for this data set was at 16 Hz.

The new warm-end heat exchanger was then installed into the apparatus. The same experimental procedure was followed except that the current to the expander was limited to 1A. This was done to preserve the operation of the expander for future experiments. There were concerns that high current to the expander could damage the unit and compromise the completion of the experiments. While current limiting the expander at 1A, low-end temperatures of 8.4 K, 8.7 K and 9.1 K were achieved at 30 Hz, 24 Hz and 16 Hz, respectively. Increasing the power to the expander would have resulted in lower temperatures at these respective frequencies. These results were much improved over the initial configuration data sets. In particular, the best results were at 30 Hz, the optimum design frequency. The results for these data are shown in Figure 8.

## CONCLUSION

Using CFD modeling to investigate improvements to the existing single-stage pulse tube cryocooler provided a heat exchanger and pulse tube design that improves flow transitioning at the warm end of the pulse tube and as a result provides lower turbulent intensity within the pulse tube which improves overall performance. Initial experimental results using the newly designed warm-end heat exchanger showed improvements in no-load cold-end temperatures at the 30 Hz design frequency while using less power to the expander to achieve lower temperatures than previous experiments demonstrated. Future experimental work will include additional pulse tube designs with non-dimensional diameters of 0.19 and 0.35. Increased power to the expander will be included to achieve optimum no-load low-end temperatures.

## ACKNOWLEDGMENT

This research was partially funded by the Office of Naval Research with Deborah Van Vechten as the project monitor.



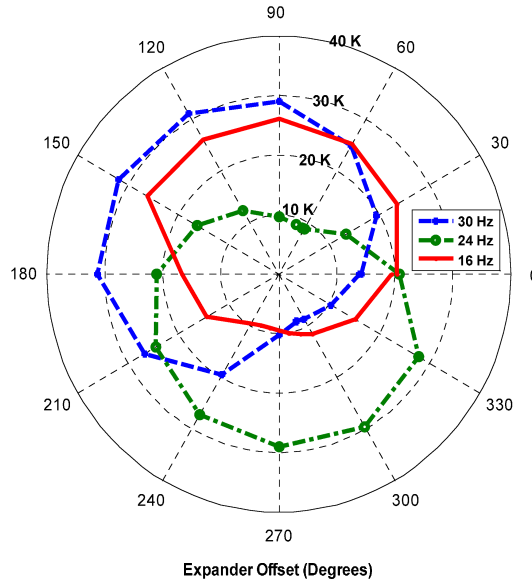


**Figure 8.** Plot showing no-load temperature of the original system with redesigned pulse tube warm heat exchanger as a function of the operating frequency and the expander offset angle; charge pressure is 1 MPa.

## REFERENCES

1. R. Radebaugh and A. O’Gallagher, “Regenerator Operation at Very High Frequencies for Microcrycoolers,” *Adv. in Cryogenic Engineering*, Vol. 51, Amer. Institute of Physics, Melville, NY (2006), pp. 1919-1928.
2. R. Radebaugh, A. O’Gallagher, and J. Gary, “Secondary Pulse Tubes and Regenerators for Coupling to Room-Temperature Phase Shifters in Multistage Pulse Tube Cryocoolers,” *Cryocoolers 16*, ICC Press, Boulder, CO (2011), pp. 237-247.
3. M.A. Lewis, P.E. Bradley, and R. Radebaugh, “Experiments with Linear Compressors for Phase Shifting in Pulse Tube Cryocoolers,” *Adv. in Cryogenic Engineering*, Vol. 57, Amer. Institute of Physics, Melville, NY (2012), pp. 1600-1607.
4. I. Garaway, M. Lewis, P. Bradley, and R. Radebaugh, “Measured and Calculated Performance of a High Frequency, 4 K Stage, He-3 Regenerator,” *Cryocoolers 16*, ICC Press, Boulder, CO (2011), pp. 405-410.
5. Taylor, R.P., *Development and Experimental Validation of a Pulse-Tube Design Tool Using Computational Fluid Dynamics*, Ph.D Thesis, The University of Wisconsin-Madison, 2009.
6. EES, *Engineering Equation Solver*, F-Chart Software., Madison, Wisconsin, 2012.
7. R. Radebaugh and V. Arp, *Isothermal Heat Exchanger*, NIST-Boulder, 1992.

